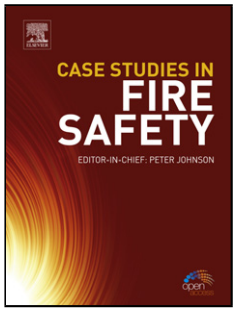

Title: Unexpected effect of citrate ions on the corrosion process of carbon steel in alkaline solutions

Authors: S. Toujas, M. Vázquez, M.B. Valcarce

PII: S0010-938X(17)30227-5
DOI: http://dx.doi.org/10.1016/j.corsci.2017.08.018
Reference: CS 7171

To appear in:

Received date: 6-2-2017
Revised date: 10-8-2017
Accepted date: 18-8-2017

Please cite this article as: S.Toujas, M.Vázquez, M.B.Valcarce, Unexpected effect of citrate ions on the corrosion process of carbon steel in alkaline solutions, Corrosion Sciencehttp://dx.doi.org/10.1016/j.corsci.2017.08.018

Unexpected effect of citrate ions on the corrosion process of carbon steel in alkaline solutions

S. Toujas, M. Vázquez and M. B. Valcarce*.

División Electroquímica Aplicada, INTEMA,

Facultad de Ingeniería, Universidad Nacional de Mar del Plata, CONICET.

J. B. Justo 4302, B7608FDQ Mar del Plata, ARGENTINA

* corresponding author

División Electroquímica Aplicada, Facultad de Ingeniería, Universidad Nacional de Mar del Plata, INTEMA, CONICET

Juan B. Justo 4302 - B7608FDQ Mar del Plata – Argentina

e-mail: mvalca@fi.mdp.edu.ar

Tel.: +54 223 481 6600 ext 244, Fax : +54 223 481 0046

Highlights:

- Citrate ions do not adsorb on passive steel in pore simulating solutions
- Citrate ions are clearly harmful to carbon steel and accelerate the corrosion process
- Citrate ions cannot be recommended as inhibiting agents for steel in pore simulating solutions

Abstract

The effect of citrate ions on the passive film stability on carbon steel, at pH 13, was evaluated. The study involved cyclic voltammograms, potentiodynamic polarization curves, micro-Raman spectroscopy and weight-loss tests. No beneficial effects on delaying or inhibiting pitting were observed in the presence of citrate ions. Organic compounds with carboxylate groups are promising corrosion inhibitors. However, the incorporation of citrate ions is clearly harmful to carbon steel in alkaline solutions and accelerates the corrosion process. Citrate ions adsorption is not observed on passive steel. Instead, citrate ions can unexpectedly dissolve the passive layer facilitating the corrosion process.

Keywords:

A) Steel reinforced concrete

B) Cyclic voltammetry; Raman spectroscopy; weight-loss.

C) Alkaline corrosion; passive films.

1. Introduction

Corrosion inhibitors have been used to prevent reinforcement bar (rebar) corrosion in concrete [1-3]. The stability of the protective passive layer naturally formed on steel can be compromised in aggressive conditions, such as those associated to concrete carbonation or chloride ions contamination. The use of simulated pore solution facilitates the control of the many factors that influence rebar corrosion and this is the approach chosen in the present investigation. The extrapolation to the behaviour of carbon steel in mortar or concrete requires additional investigation.

Organic compounds with carboxylate group have been presented as promising corrosion inhibitors of carbon steel in high alkaline media contaminated with chloride ions [4-7]. Ormellese and col. [6] studied different organic compounds with carboxylate groups using anodic polarization curves. Citrate ions were presented as good pitting inhibitors, as they could adsorb on the bare metal (without a passive layer), avoiding chloride ions adsorption due to a steric effect. However, citrate ions present a chelating effect, forming soluble complexes with Fe(II) and Fe(III) [8]. Nevertheless, other authors proposed that organic compounds with carboxylate groups suppress the formation of a $Fe_3O_4/\gamma\text{-}Fe_2O_3$ bilayer passive film in borax pH 8.4, by forming a soluble Fe(II)-complex. This avoids oxidation to Fe(III) and subsequently, prevents Fe(III) oxo/hydroxide formation in the passive layer [9]. In particular, citrate ions increase the active dissolution of carbon steel in borax pH 8.4 [10]. In addition, passivated iron weakens the adsorption of carboxylate groups, which is stronger on bare iron (active) [11]. Citrate ions could adsorb on bare surfaces to prevent chloride ions adsorption but the presence of a passive layer (a more realistic service condition) could interfere in this competition. Furthermore, the protective passive layer could suffer a detrimental effect in the presence of citrate ions. Hence, the effectivity of citrate ions as potential

corrosion inhibitors at pH 13 (typical of concrete) needs to be evaluated. The aim of this work is to study the stability of a passive film on carbon steel in a concrete pore simulated solution (pH=13) contaminated with chloride ions when citrate ions are also present.

2. Materials and methods

2.1. Electrodes preparation

Reinforcement bars were used to cut disks, embed them in acrylic resin and prepare the electrodes with appropriate back contacts. Average composition is as follows: Mn 0.635 wt%, C 0.299 wt%, Si 0.258 wt%, Cu 0.227 wt% and others impurities 0.245 wt %. The exposed area was 0.503 cm^2. The surfaces were abraded with 1000 emery paper.

2.2. Electrolyte composition

A pH 13 pore simulating solution (PSS) was used as electrolyte, containing KOH 0.08 mol/L, NaOH 0.02 mol/L and $Ca(OH)_2$ 0.001 mol L^{-1} [12]. To evaluate the effect of chloride and citrate ions (cit), NaCl 0.3 mol L^{-1} and $C_6H_5Na_3O_7.2H_2O$ 0.15 and 0.3 mol L^{-1} were incorporated. In order to compare to the behaviour of a corrosion inhibitor frequently used in concrete, PSS incorporating 0.3 mol L^{-1} nitrite ions were also tested [13-16].

2.3. Electrochemical techniques

A conventional three-electrode cell was used. As reference electrode a mercuric oxide Hg/HgO electrode was employed (MOE, 1 mol L^{-1} KOH solution, E = 0.123 V_{NHE}). All the potential values will be referred to this electrode. The auxiliary electrode was a platinum wire. Electrochemical tests were carried out using a Voltalab PGZ 100 potentiostat in stagnant solutions.

Cyclic voltammograms were recorded at 10 mV s^{-1} in deaerated electrolytes after pre-reducing 5 minutes at −1.2 V_{MOE}.

The corrosion potential (E_{CORR}) was followed during 24 h in each condition investigated. Not less than five individual measurements were registered and averaged.

Polarization resistance (R_P) was calculated as $\Delta V/\Delta i$, from potential sweeps at 0.1 mV s^{-1} scanning ± 0.015 V from the E_{CORR}.

Anodic polarization curves were registered at 0.1 mV s^{-1} using two different starting conditions: a) bare metal (electrodes pre-reduced for 5 minutes at −1.2 V_{MOE}); b) passivated electrodes (aged for 24 h at E_{CORR}). Each potentiodynamic scan started at the pre-treatment potential. The scan direction was inverted when reaching 100 µA cm^{-2}. The experiments were designed according to the ASTM norms [16]. After these tests, the electrodes were dried under N_2 to register Raman spectra of the corrosion products.

Tests were performed at ambient temperature (20 ± 2 ºC).

2.4. Weight loss determinations

Weight-loss tests were performed as recommended in ASTM D 2688 [17]. Disks with 5.67 cm^2 as geometrical area were cut from the rebars and abraded with grade 120 emery paper. Weighted coupons were immersed for 90 days in PSS, PSS + Cl^- , PSS + *[*cit*]*/*[*Cl^-*]*=0.5 and PSS + *[*cit*]*/*[*Cl^-*]*=1. Three coupons were simultaneously immersed at room temperature in each flask. One of them was dried under N_2 atmosphere to record *ex-situ* Raman spectra on the corroded surface. The other two coupons were cleaned by immersion in HCl 1 mol L^{-1}, and then neutralized with a Na_2CO_3 saturated solution, rinsed with distilled water, dried and weighted.

2.5. Ex-situ Raman spectra

The Raman measurements were recorded using a 514 nm laser and an Invia Reflex confocal Raman microprobe. Settings were chosen as reported before [12]. At least five representative spots were evaluated and observed to be reproducible.

3. Results

3.1. Electrochemical evaluation on bare metal

3.1.1 Cyclic voltammetry

Figure 1 presents the first cycle of the cyclic voltamograms performed in PSS, PSS + Cl^- and PSS + $[cit]/[Cl^-]$=1. The curves in PSS and in PSS + Cl^- were described in more detail in a previous work [12]. The discussion of those results is summarised here so as to compare with the effect of citrate ions. In PSS, the four anodic peaks have been previously described by different authors [12, 19-22]. The first anodic peak at -0.92 V_{MOE} (Ia) has been associated to the oxidation of hydrogen atoms formed during pre-reduction. Then, peak IIa at -0.74 V_{MOE} has been attributed to the formation Fe_3O_4 together with hydrated Fe(II) and Fe(III) species. Peak IIIa at -0.6 V_{MOE} corresponds to $Fe(OH)_3$ and/or α- or δ-FeOOH. Peak IVa at -0.30 V_{MOE} involves $Fe(OH)_2$ transforming into $Fe(OH)_3$ or γ-FeOOH [20]. The two cathodic peaks registered in PSS, Ic at -0.69 V_{MOE} and IIc at -0.89 V_{MOE}, are associated to the reduction of Fe(III) and Fe(II) species, respectively. The total reduction charge is lower than the oxidation charge because the inner magnetite layer is quite insoluble and prevents further dissolution of the outer part of the surface film [20, 21].

When chloride ions are added (PSS + Cl^-), four oxidation peaks appear at the same potentials observed in PSS (see Figure 1). Peaks IIa and IIIa are more intense because iron is readily oxidized when chloride ions are present in the electrolyte. Also, as iron

oxides and hydroxides are more soluble in SSP + Cl^-, there is only one reduction peak [23].

In PSS + *[*cit*]*/*[*Cl^-*]*=1, the anodic sweep can extend to potential values higher than those reached in PSS + Cl^-. The intensity of peak IIIa decreases compared to that of PSS + Cl^- probably due to the lower concentration of Fe(II) species present on the metal surface. Even if it is possible to continue the sweep until 0.5 V_{MOE} without observing localized attack, the current density at potentials higher than -0.5 V_{MOE} is higher in the presence of citrate ions. This increment in the current could be associated to the formation of an iron-citrate soluble complex resulting from the dissolution of the protective iron oxide [10]. After reversing the scan, one anodic peak at 0 V_{MOE} could be observed. This peak has been observed before in the presence of citrate ions on steel [10, 24]. It has been related to Fe(II) species in solution, suggesting that the passive layer is partially soluble in citrate-rich media.

Figure 2 shows the 10^{th} cycle of the voltammograms recorded in PSS, PSS + Cl^- and PSS + *[*cit*]*/*[*Cl^-*]*=1 . In PSS and PSS + Cl^- , one anodic peak (IIIa) at -0.6 V_{MOE} and one cathodic peak (Ic) can be observed, in agreement with results from other authors [20, 21]. The charge of these two peaks increases progressively with each new cycle [12,19, 20, 25] (results not shown) and can be explained by the growth of corrosion products on the metal surface, as the inner layer of magnetite is never completely reduced. In contrast, when citrate ions are incorporated, the charges corresponding to the anodic (IIIa) and the cathodic peak (Ic) remain almost constant with cycling. This behaviour could be related to the formation of a soluble Fe(II)-complex which would leave a lower amount of iron(II) compounds available to be oxidized within the potential range associated to peak IIIa [19]. In the presence of citrate ions, the potential can be scanned up to 0.5 V_{MOE} without observing localized attack, even after ten cycles. In the first

cycle (Figure 1) oxidation of soluble Fe(II) compounds was observed. However after cycling, this peak is no longer visible, probably due to the development of a compact oxide layer on the metal surface which limits dissolution. However, the current density at potentials higher than -0.5 V_{MOE} is, for this condition, the highest. This behaviour suggests that citrate ions have two different effects depending on the composition of the metal/electrolyte interface: they could adsorb on bare iron desorbing chloride ions and preventing localized attack. In parallel, on a passive surface, citrate ions could favour Fe(II) dissolution producing a superficial layer with properties that are very different than those found in PSS and PSS + Cl^- [9].

3.1.2. Anodic polarization curves

Figure 3 presents the polarization curves of bare carbon steel in PSS + Cl^- and PSS + *[*cit*]/[*Cl^-*]*=1. The electrodes were pre-treated at -1.2 V_{MOE}.

In SPP + Cl^-, the region between -1.2 and -0.4 V_{MOE}, corresponds to the cathodic branch (oxygen reduction). A pseudo passivity current of 5 mA cm^{-2} is registered, together with a pseudo-pitting potential of -0.08 V_{MOE}. In PSS + *[*cit*]/[*Cl^-*]*=1, the cathodic range extends from -1.2 to -0.7 V_{MOE}. At potentials higher than -0.5 V_{MOE}, a decrease in the current density as the potential is scanned in the positive direction could be indicating the formation of a protective surface film. This protective layer could be either an oxide layer growing on the alloy's surface, an adsorpted layer of citrate ions on the alloy, or both. The positive end of the potential sweep may reach values higher than 0.5 V_{MOE} without any signs of localized attack. These results are in agreement with those presented by other authors for organic substances with mono and poli-carboxilate groups such as sodium citrate [6, 7]. These findings show the beneficial effects of citrate ions in delaying localized attack. Citrate ions could adsorb on bare metal surfaces

competing with chloride ion adsorption. However, in real service conditions, carbon steel embedded in concrete is in an alkaline environment and presents a passive surface, with an oxide layer existing on top of bare material.

3.2. Electrochemical evaluation on the passive metal

The electrodes were aged 24 h at E_{CORR} because this condition represents a closer approach to the service condition in which steel bars exposed to the atmosphere for long periods of time are embedded in concrete.

3.2.1. Corrosion potentials

Corrosion potentials values were found to be constant and stable after 24 h. Table 2 shows values obtained in each case as an average of not less than three independent measurements. The values obtained for each different condition are typical of passive steel, as discussed before [12].

3.2.2. Linear polarization resistance

The R_P values were calculated using the linear polarization resistance method (LPR). The slope (dE/di) at zero-current potential is the polarization resistance. Table 2 shows the results for R_P measurements after 24 h at E_{CORR}. It can be seen that the R_P values are close to 100 kΩ cm^2 in PSS + Cl^-, PSS + $[cit]/[Cl^-]$=0.5 and $[NO_2^-]/[Cl^-]$=1. This value is typical of passive electrodes [26-28]. But surprisingly, when the citrate content increases in a factor of 2 (PSS + $[cit]/[Cl^-]$=1), the polarization resistance decreases 3 times. In the presence of a high concentration of citrate ions, R_P values end up being

close to those typical of carbon steel in active dissolution (lower than 10 kΩ cm^2) [26-28].

3.2.3 Anodic Polarization Curves

Figure 4 shows the anodic polarization curves registered after ageing the electrodes 24 h at E_{CORR} in PSS, PSS + Cl^-, PSS + *[*cit*]*/*[*Cl^-*]*=0.5, PSS + *[*cit*]*/*[*Cl^-*]*=1 and PSS + *[*NO_2^-*]*/*[*Cl^-*]*=1. Electrochemical parameters such as passivity current densities (i_{PAS}) and pitting potentials (E_{PIT}) were calculated from an average of not less than 6 anodic polarization curves and are presented in Table 3.

In PSS, carbon steel remains passive with the lowest i_{PAS} registered [12]. When chloride ions are incorporated into the electrolyte, pitting is observed at potentials around 0.06 V_{MOE} together with an increment in i_{PAS}.

The highest E_{PIT} (higher than 0.6 V_{MOE}) together with the highest difference (E_{PIT}-E_{CORR}) were registered in PSS + *[*NO_2^-*]*/*[*Cl^-*]*=1. In addition, the i_{PAS} measured when nitrites and chlorides are present is close to that measured in PSS. This behaviour is characteristic of this type of anodic inhibitor in alkaline solutions heavily contaminated with chloride ions [27]. After reversing the sweep, the current density decreases up to 4 μA cm^2 in the proximity of E_{CORR}. This would indicate a beneficial effect of nitrite ions on the repassivation process inside of the pit [15].

When citrate ions are used instead of nitrites, no significant differences were observed on E_{PIT} and (E_{PIT}-E_{CORR}) when compared to PSS + Cl^- . No beneficial effects of citrate ions were observed on localized attack. Conversely, i_{PAS} increases by a factor of 2 for the highest citrate ion concentration tested. This would indicate a detrimental effect of citrate ions on the passive film. Citrate ions seem to favour Fe(II)-oxide dissolution producing a less compact and more unstable passive film [9, 10, 29].

Images of the electrode surfaces after having performed the anodic polarization curves in PSS + *[*cit*]*/*[*Cl^-*]*=1 (A) and PSS + Cl^- (B) are presented in Figure 5. In both conditions, pitting attack is observed. However the corrosion products look different. The black corrosion product when citrate ions are present indicates the participation of Fe_3O_4; while in PSS + Cl^- corrosion products are red, indicating the presence of iron(III) oxide/hydroxide.

3.3. Weight loss tests

The effect of citrate ions on the passive film stability at longer times was also evaluated. Weight-loss tests lasted 90 days, as described in detail in section 2.4. The corrosion current density (i_{CORR}) in each condition was calculated using Faraday's law [30]

$$i_{CORR} = \frac{m F z}{A t M} \qquad (3)$$

where m represents the mass lost, F accounts for the Faraday constant, A is the exposed area, t is the exposure time, M is the atomic mass and *z* is the electron number (taken as 2). The calculated values for the corrosion current density are presented in Table 4. Figure 6 shows images of the coupons after the immersion and cleaning stages. As expected, in PSS no attack or corrosion products were detected. Weight loss was negligible and the i_{CORR} is typical of passive carbon steel [12, 31, 32]. In contrast, an important degree of pitting attack is evident on the coupons immersed in PSS + Cl^-, accompanied by a noticeable increment in i_{CORR}. Abundant red corrosion products were striped by chemical cleaning before the coupons were weighted. No sign of localized corrosion was observed on the surface of the coupons immersed in PSS + *[*NO_2^-*]*/*[*Cl^-*]*=1. As in PSS, the calculated values for i_{CORR} turned out to be typical of passive steel, even after the coupons were immersed for 90 days in a chloride-containing electrolyte.

As regards citrate ions, pitting was observed in both PSS + *[*cit*]*/*[*Cl^-*]*=1 and PSS + *[*cit*]*/*[*Cl^-*]*=0.5, after 90 days of immersion. The mass lost in the presence of citrate ions was the highest. Also the attack was more severe when the citrate ions concentration increased. The i_{CORR} value in PSS + *[*cit*]*/*[*Cl^-*]*=1 was four times higher than in PSS + Cl^-. There were some black corrosion products present on the coupons before chemical cleaning. However, after removal of these black corrosion products, many holes could be observed (see Figure 6). In addition, to evaluate the effect of citrate ions itself, the weight-loss test was repeated in PSS + cit. After 90 days, and even when no chloride ions were present in this condition, pitting attack was observed after removing the corrosion products. The i_{CORR} in PSS + cit was three times higher than in PSS + Cl^-, showing that citrate ions acted as pitting promoting agents, as chloride ions did.

3.4. Raman confocal spectroscopy

Ex-situ Raman spectra were registered to characterize corrosion products and passive films in two conditions: after accelerating the pitting process by anodic polarization and after performing the weight-loss tests. These measurements require a relatively high laser power, given that the most common iron oxides and oxyhydroxides are poor light scatters [33]. Precautions were taken so as not to induce chemical changes by laser heating. Figure 5 shows images of the steel surfaces after having registered anodic polarization curves in PSS + Cl^- and PSS + *[*cit*]*/*[*Cl^-*]*=1. Raman spectra of the surface products are presented in Figure 7. Bands at 220, 280, 395 and 595 cm^{-1} in spectrum **B** are typical of α-FeOOH and/or α-Fe_2O_3 [19, 27, 34]. The band at 680 cm^{-1} can be associated to the presence of Fe_3O_4 [19, 27, 34]. In spectrum **A**, the band at 680 cm^{-1}, related to Fe_3O_4, can be also observed, but the bands characteristic of α-FeOOH and/or α-Fe_2O_3 were not clearly observed.

Raman spectra of the corrosion products, before chemically cleaning the coupons, and after the weight-loss tests in PSS + Cl^- and PSS + *[*cit*]/[*Cl^-*]*=1 are presented in Figure 8. Also, the Raman spectrum of the passive film present in PSS + *[*NO_2^-*]/[*Cl^-*]*=1 is shown in Figure 8 for comparison. These results agree with those presented in Figure 7, which evaluated the surface after recording anodic polarization curves. In the case of PSS + Cl^-, bands associated to α-FeOOH and/or α-Fe_2O_3 are present, indicating the participation of Fe(III) oxides/oxyhydroxides in the red corrosion products. When nitrite ions are present there is no evidence of sharp bands in this spectrum, except for a poorly defined band at 280 cm^{-1} related to the main band of α-FeOOH. The fact that no characteristic signals were observed could be explained if a very thin passive film were present on the steel surface. Also, iron oxides or oxo-hydroxides could be present as a disordered or amorphous structure, hindering a clear identification [34]. In PSS + *[*cit*]/[*Cl^-*]*=1, the characteristic signal of α-FeOOH and Fe_3O_4 was not observed. Instead, a band at 680 cm^{-1} related to the presence of Fe_3O_4 was observed, indicating a poor participation of Fe(III) oxide/hydroxide in the black corrosion products.

4. Discussion

In PSS carbon steel remains passive and when chloride ions are incorporated pitting attack is triggered. Nitrite ions behave as efficient inhibiting agents and are able to overcome the presence of chloride ions.

Instead, in the presence of citrate ions, the properties of the passive layer are very different than those developed in PSS and PSS + Cl^-. The effect is just the opposite to that expected for an inhibitor, as citrate ions favour the dissolution of the passive film.

As Fe(II) compounds dissolve, no Fe(III) oxide/hydroxide incorporates to the passive film. Polarization curves with electrodes aged 24 h at E_{CORR} show passive behaviour, but with a high corrosion density value, in agreement with the low R_P values measured. No beneficial effects on delaying or inhibiting pitting were observed in the presence of citrate ions. These short-term results are in agreement with weight-loss analysis. After 90 days of exposure, the highest weight-loss registered was that in PSS + $[cit]/[Cl^-]$=1, together with severe pitting attack. Weight-loss was 3.7 times higher than that found in PSS + Cl^-. To confirm the effect of citrate ions a weight-loss test without chloride ions was included in the analysis. In PSS + $[cit]/[Cl^-]$=1, the weight lost was higher than that found for PSS + cit and for PSS + Cl^-. This indicates a synergic effect between chloride and citrate ions in the deterioration of the protective passive layer. Raman spectra recorded after the anodic polarization curves and weight-loss tests show, that in the presence of citrate ions, black corrosion products are mainly composed by Fe_3O_4.

The incorporation of citrate ions to PSS + Cl^- is clearly harmful to carbon steel and favours the corrosion process. However, some authors [6, 7] have pointed out that organic compounds with carboxylate groups, could act as pitting inhibitors in alkaline solutions. However, the conditions used to evaluate them as potential inhibitors are similar to those employed in section 3.1.2, namely no passive film is present. Under this condition, citrate ions could adsorb on the bare metal while the electrodes are polarized, hindering the access of chloride ions to the metal surface. At highly anodic potentials this adsorbed layer could break locally. On the other hand, if citrate ions are not present, an oxide layer grows while the electrode is polarized. Eventually, as this is a chloride-rich environment, this surface layer break down leading to pitting attack at lower potentials than those registered in the presence of citrate ions. However, after a 24 h immersion at E_{CORR}, a passive layer grows on metal surface which inhibits citrate ions

adsorption. In contrast, citrate ions favour iron dissolution forming soluble iron-complexes and producing a superficial layer of corrosion products that is porous, poorly adhered and unable to provide protection against localized attack.

5. Conclusions

1. In alkaline solutions that simulate the contents of concrete pores, carbon steel remains passive. When a passivating film is present on the steel surface, citrate ion do not seem to adsorb.
2. Under these conditions, citrate ions do not function as corrosion inhibitor. Instead, and by contrast, citrate ions enhance dissolution of the passive layer, thereby accelerating the corrosion process. This was unexpected.
3. When the steel surface is pre-passivated, a synergic effect between chloride and citrate ions that leads to the deterioration of the protective passive layer was observed.
4. In spite of being an organic compound with carboxylate groups, citrate ions behave as corrosion accelerators, instead of acting as inhibiting agents.
5. During the evaluation of potential inhibiting agents it is then very important to use conditions that mimic the real service environment as closely as possible. In the case of steel in concrete, a real service condition involves a passive surface and long exposure times.

Acknowledgments

This work has been supported by the University of Mar del Plata (Grant 15/G450), as well as by the National Research Council (CONICET, PIP0670).

References

[1] B. Elsener, Corrosion inhibitors for steel in concrete. State of the art report, Maney Publishing, London, 2001.

[2] J.M. Gaidis, Chemistry of corrosion inhibitors, Cem. Concr. Compos., 26 (2004) 181.

[3] C.M. Hansson, L. Mammoliti, B.B. Hope, Corrosion inhibitors in concrete--part I: the principles, Cement and Concrete Research, 28 (1998) 1775-1781.

[4] S. Muralidharan, V. Saraswathy, K. Thangavel, S. Srinivasan, Competitive role of inhibitive and aggresive ions in the corrosion of steel in concrete, J. Appl. Electrochem., 30 (2000) 1255-1259.

[5] S. Muralidharan, V. Saraswathy, S.P.M. Nima, N. Palaniswamy, Evaluation of a composite corrosion inhibiting admixtures and its performance in Portland pozzolana cement, Mater. Chem. Phys., 86 (2004) 298-306.

[6] M. Ormellese, L. Lazzari, S. Goidanich, G. Fumagalli, A. Brenna, A study of organic substances as inhibitors for chloride-induced corrosion in concrete, Corros. Sci., 51 (2009) 2959-2968.

[7] S. Martinez, L. Valek, I.s. Oslakovic, Adsorption of organic anions on low-carbon steel in saturated $Ca(OH)_2$ and the HSAB principle., Journal of Electrochemical Society, 154 (2007) C671-C677.

[8] A. Bino, I. Shweky, S. Cohen, E.R. Bauminger, S.J. Lippard, A Novel Nonairon(III) Citrate Complex: A “Ferric Triple-Decker”, Inorg. Chem., 37 (1998) 5168-5172.

[9] E. Sikora, D. Macdonald, The passivity of iron in the presence of ethylenediaminetetraacetic acid I. General electrochemical behaviour., J. Electrochem. Soc., 147 (2000) 4087-4092.

[10] S. Modiano, C.S. Fugivara, A.V. Benedetti, Effect of citrate on the electrochemical behaviour of low-carbon steel in borate buffer solutions, Corros. Sci., 46 (2004) 529-545.

[11] P. Kern, D. Landolt, Adsorption of organic corrosion inhibitors on iron in the active and passive state. A replacement reaction between inhibitor and water studied with rotating quartz crystal microbalance., Electrochim. Acta, 47 (2001) 589-598.

[12] L. Yohai, M. Vázquez, M.B. Valcarce, Phosphate ions as corrosion inhibitors for reinforcement steel inchloride-rich environments, Electrochim. Acta, 102 (2013) 88-96.

[13] A.M. Rosemberg, J.M. Gaidis, The mechanism of nitrite inhibition of chloride attack on reinforcing steel in alkaline aqueous environments, Mater. Perform., 18 (1979) 45.

[14] P. Garcés, P. Saura, E. Zornoza, C. Andrade, Influence of pH on the nitrite corrosion inhibition of reinforcing steel in simulated concrete pore solution, Corros. Sci., 53 (2011) 3991-4000.

[15] S.M.A.E. Haleem, S.A.E. Wanees, E.E.A.E. Aal, A. Diab, Environmental factors affecting the corrosion behavior of reinforcing steel. IV. Variation in the pitting corrosion current in relation to the concentration of the aggressive and the inhibitive anions, Corros. Sci., 52 (2010) 1675-1683.

[16] M.B. Valcarce, M. Vázquez, Carbon steel passivity examined in alkaline solutions: The effect of chloride and nitrite ions, Electrochim. Acta, 53 (2008) 5007-5015.

[17] American Society of Testing and Materials, ASTM G61-86, Philadelphia, 1993.

[18] American Society of Testing and Materials, ASTM D2688, Philadelphia, 1993.

[19] A. Hugot-Le Goff, J. Flis, N. Boucherit, S. Joiret, J. Wilinski, Use of Raman spectroscopy and rotating split ring disk electrode for identification of surface layers on iron in 1M NaOH, J. Electrochem. Soc., 137 (1990) 2684-2690.

[20] W. Xu, K. Daub, X. Zhang, J.J. Noel, D.W. Shoesmith, J.C. Wren, Oxide formation and conversion on carbon steel in mildly basic solutions, Electrochim. Acta, 54 (2009) 5727-5738.

[21] X. Zhang, W. Xu, D.W. Shoesmith, J.C. Wren, Kinetics of H_2O_2 reaction with oxide films on carbon steel, Corros. Sci., 49 (2007) 4553-4567.

[22] S. Joiret, M. Keddam, X.R. Novoa, M.C. Perez, C. Rangel, H. Takenouti, Use of EIS, ring-disk electrode, EQCM and Raman spectroscopy to study the film of oxides formed on iron in 1M NaOH, Cem. Con. Comp., 24 (2002) 7 - 15.

[23] P. Ghods, O.B. Isgor, J.R. Brown, F. Bensebaa, D. Kingston, XPS depth profiling study on the passive oxide film of carbon steel in saturated calcium hydroxide solution and the effect of chloride on the film properties, Appl. Surf. Sci., 257 (2011) 4669-4677.

[24] H. Hassan, Effect of chloride ions on the corrosion behaviour of steel in 0.1 M citrate, Electrochim. Acta, 51 (2005) 526-535.

[25] P. Schmuki, M. Buchler, S. Virtanen, H.S. Isaacs, M.P. Ryan, H. Bohni, Passivity of iron in alkaline solutions studied by in situ XANES and a laser reflection technique, Journal of Electrochemical Society, 146 (1999) 2097-2102.

[26] J.A. González, J.M. Miranda, N. Birbilis, S. Feliu, Electrochemical techniques for studying corrosion of reinforcing steel: limitations and advantages, Corrosion, 61 (2005) 37-49.

[27] M.B. Valcarce, C. López, M. Vázquez, The Role of Chloride, Nitrite and Carbonate Ions on Carbon Steel Passivity Studied in Simulating Concrete Pore Solutions, J. Electrochem. Soc., 159 (2012) C244.

[28] M.F. Montemor, A.M.P. Simoes, M.G.S. Ferreira, Chloride-induced corrosion on reinforcing steel: From the fundamentals to the monitoring techniques, Cem. Con. Comp., 25 (2003) 491-502.

[29] H. Harms, H. Volkland, G. Repphun, A. Hiltpolt, O. Wanner, A.J.B. Zehnder, Action of chelators on solid iron in phosphate-containing aqueous solutions, Corros. Sci., 45 (2003) 1717-1732.

[30] American Society of Testing and Materials, ASTM G102-89, Standard Practice 624 for Calculation of Corrosion Rates and Related Information from Electrochem- 625 ical Measurements. , Philadelphia., 1994.

[31] J.A. Gonzalez, E. Ramirez, A. Bautista, S. Feliu, The behaviour of pre-rusted steel in concrete, Cem. Con. Res., 26 (1996) 501-511.

[32] A. Poursaee, C.M. Hansson, Reinforcing steel passivation in mortar and pore solution, 37, (2007) 1127–1133.

[33] D.L.A. de Faria, S. Venancio Silva, M.T. de Oliveira, Raman Microspectroscopy of Some Iron Oxides and Oxyhydroxides, J. Raman Spectrosc., 28 (1997) 873-878.

[34] B. Díaz, S. Joiret, M. Keddam, X.R. Nóvoa, M.C. Pérez, H. Takenouti, Passivity of iron in red mud's water solutions, Electrochim. Acta, 49 (2004) 3039-3048.

Figure captions

Figure 1. Cyclic voltammograms for carbon steel (first cycle) in PSS (—), PSS + Cl^- **(–Δ–);** PSS + *[*cit*]*/*[*Cl^-*]*=1 **(–○–).** Sweep rate: 10 mV s^{-1}.

Figure 2. Cyclic voltammograms for carbon steel (tenth cycle) in PSS (—), PSS + Cl^- **(–Δ–);** PSS + *[*cit*]*/*[*Cl^-*]*=1 **(–○–).** Sweep rate: 10 mV s^{-1}.

Figure 3. Anodic polarization curves registered after pre-reducing carbon steel electrodes 5 minutes at −1.2 V_{MOE} (bare metal) in PSS + Cl^- **(–Δ–)** and PSS + *[*cit*]*/*[*Cl^-*]*=1 **(–○–).** Sweep rate: 0.1 mV s^{-1}.

Figure 4. Anodic polarization curves registered after ageing carbon steel electrodes for 24 h at the E_{CORR} (passivated metal) in PSS (—), PSS + Cl^- (–Δ–); PSS + *[*cit*]*/*[*Cl^-*]*=1 (–○–); PSS + *[*cit*]*/*[*Cl^-*]*=0.5 (–□–) and PSS + *[*NO_2^-*]*/*[*Cl^-*]*=1 (-∗-).

Figure 5. Images of the electrodes' surface after carrying out the anodic polarization curves on passivated carbon steel in PSS + *[*cit*]*/*[*Cl^-*]*=1 (A) and PSS + Cl^- (B). Electrode exposed area: 0.503 cm^2.

Figure 6. Images of the coupons' surface, after being immersed for 90 days at E_{CORR} in each electrolyte (as indicated). Coupons exposed area: 5.67 cm^2.

Figure 7. Raman spectra of corrosion products on passivated electrodes after performing anodic polarization curves in (A): PSS + *[*cit*]*/*[*Cl^-*]*=1 and (B): PSS + Cl^- .

Figure 8. Raman spectra of corrosion products in PSS + Cl^- (–Δ–) and PSS + *[*cit*]*/*[*Cl^-*]*=1 **(–○–)**. Raman spectra of passivated carbon steel in PSS + *[*NO_2^-*]*/*[*Cl^-*]*=1 (-∗-). Coupons were immersed for 90 days in each electrolyte at E_{CORR}.

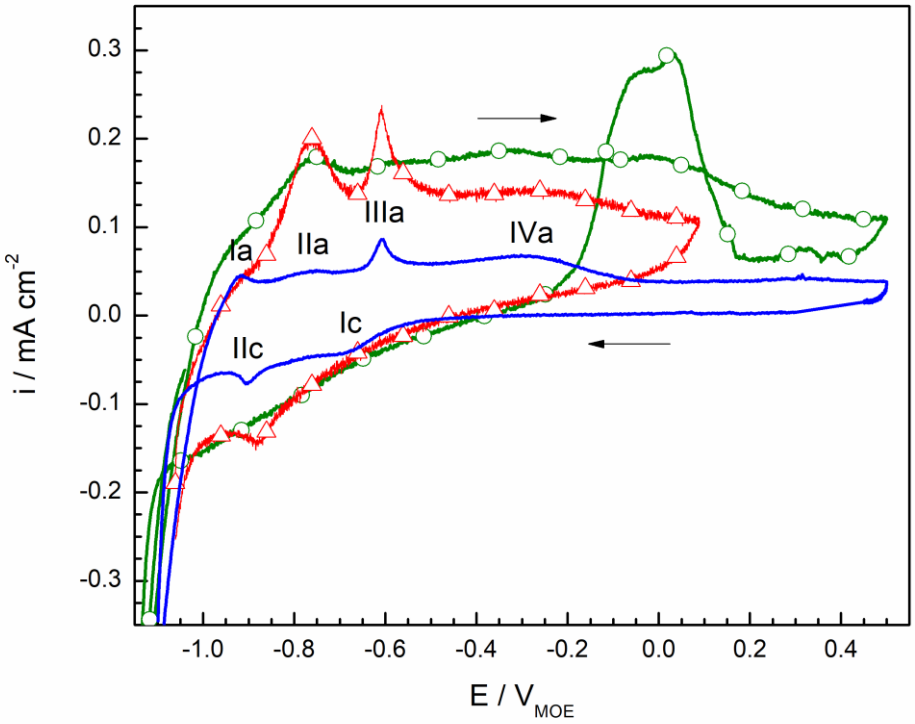

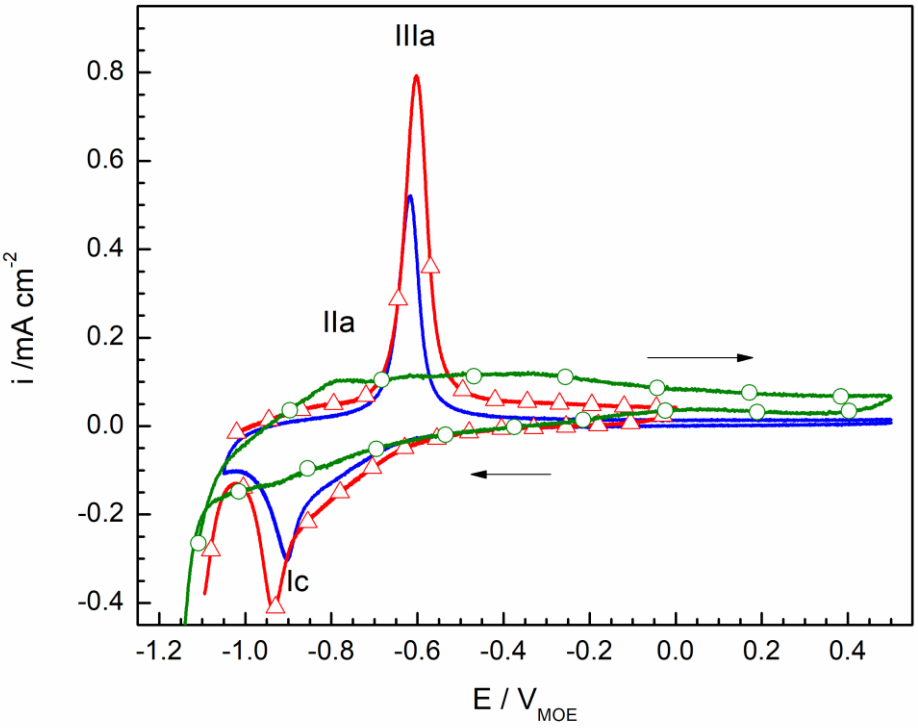

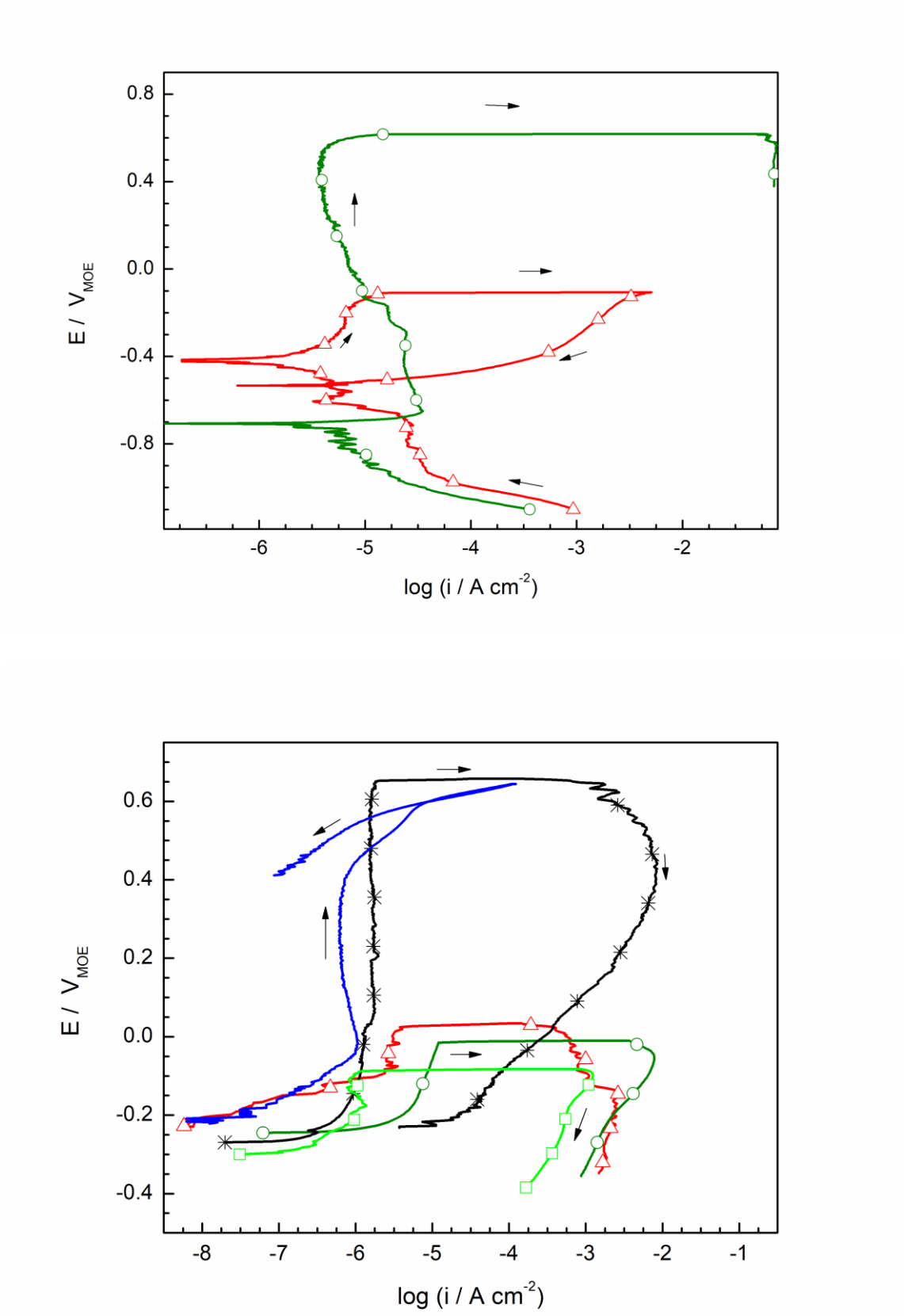

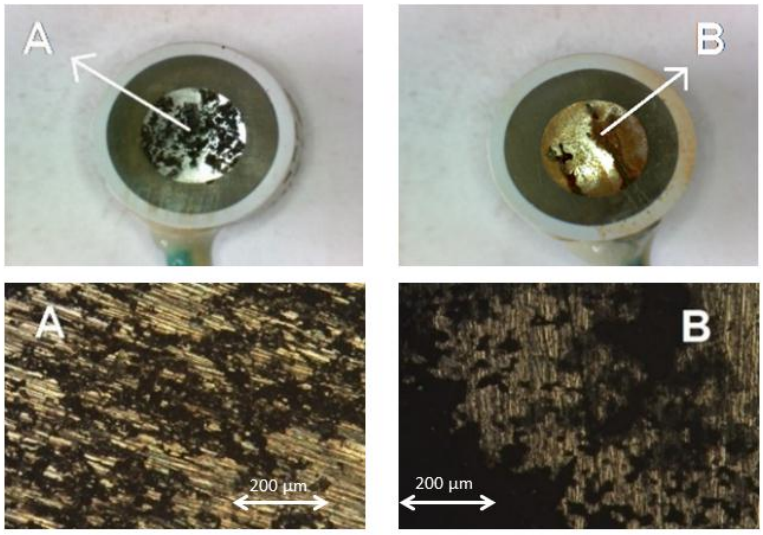

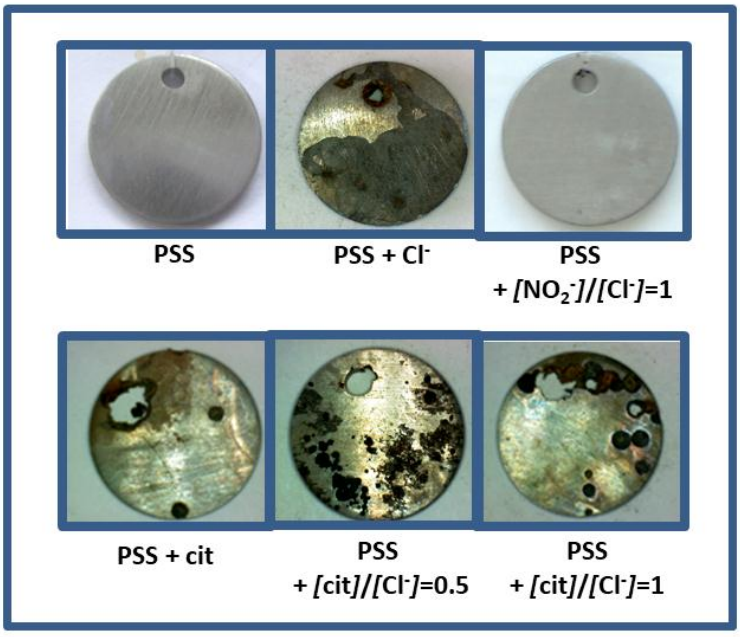

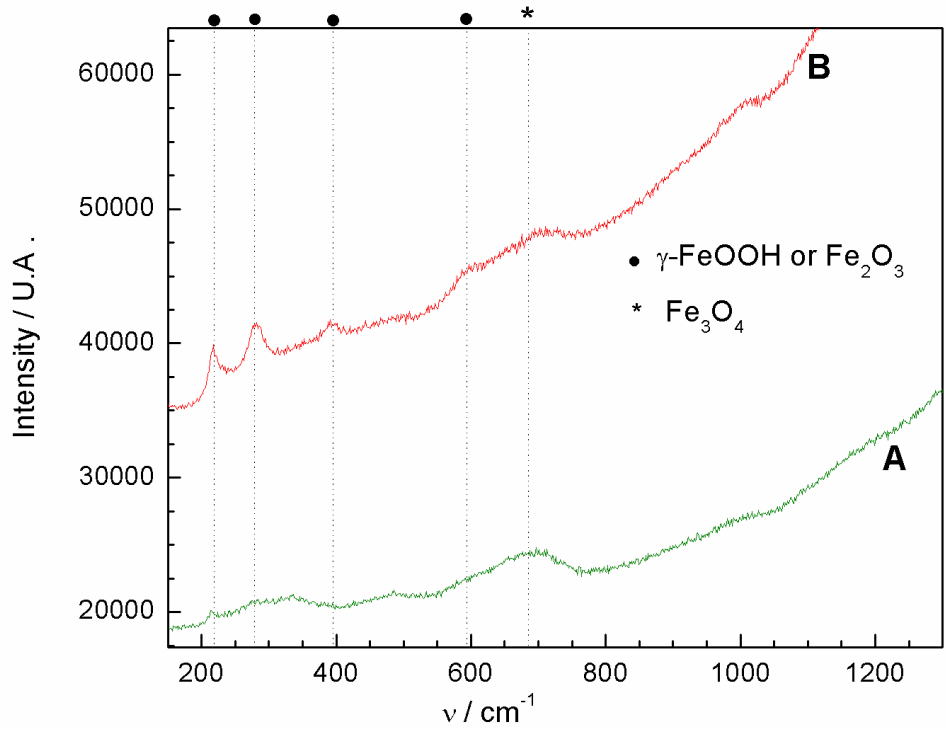

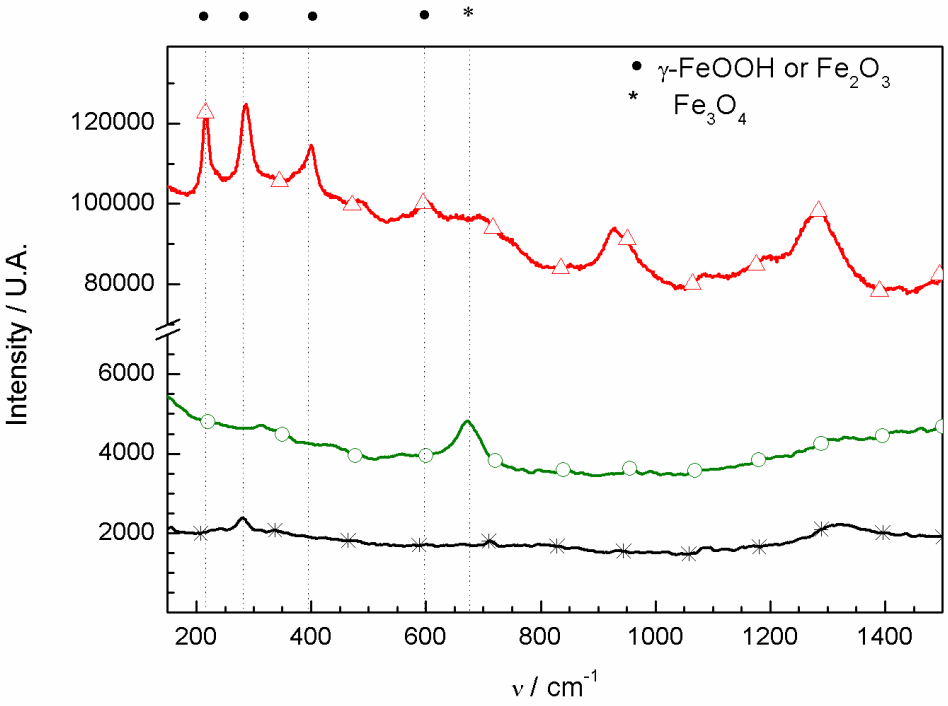

Table 1. Corrosion potential and Rp values, evaluated after 24 h of immersion in each solution.

	PSS + Cl^-	**PSS + *[cit]*//*[Cl^-]*=0.5**	**PSS + *[cit]*//*[Cl^-]*=1**	**PSS + *[NO_2^-]*//*[Cl^-]*=1**
E_{CORR} / mV_{MOE}	-229 ± 51	-300 ± 87	-250 ± 82	-268 ± 90
R_P / kohm cm^2	86 ± 15	93.1 ± 18	28.9 ± 7	78.1 ± 25

Table 2. Corrosion potentials and polarization resistance values evaluated from LPR, after 24 h of immersion in each solution.

	PSS + Cl^-	**PSS + *[cit]*//*[Cl^-]*=0.5**	**PSS + *[cit]*//*[Cl^-]*=1**	**PSS + *[NO_2^-]*//*[Cl^-]*=1**
E_{CORR} / mV_{MOE}	-229 ± 51	-300 ± 87	-250 ± 82	-268 ± 90
R_P / kohm cm^2	86 ± 15	93.1 ± 18	28.9 ± 7	78.1 ± 25

Table 3. Electrochemical parameters obtained from at least six anodic polarization curves for steel in the conditions evaluated.

Condition	E_{CORR} / mV_{MOE}	E_{PIT} / mV_{MOE}	E_{PIT}-E_{CORR} / mV	i_{PAS}/ µA cm^{-2}
PSS	-208 ± 22	---------	---------	0.7 ± 0.1
PSS + Cl^-	-229 ± 51	6 ± 64	182 ± 81	5.4 ± 2.6
PSS+ *[cit]*//*[Cl^-]*=0.5	-300 ± 87	-14 ± 8	286 ± 53	2.8 ± 1.8
PSS+ *[cit]*//*[Cl^-]*=1	-250 ± 82	-16 ± 42	227 ± 64	9.3 ± 5.8
PSS+ *[Cl^-]*//*[NO_2^-]*=1	-268 ± 90	658 ± 55	926 ± 87	1.7 ± 1.1

Table 4. Weight loss result after 90 days of immersion at E_{CORR} in the different solutions tested

Condition	Type of attack	Weight loss / mg	i_{CORR} / µA cm^{-2}
PSS	None	0.1	0.006
PSS + Cl^-	Pitting	110	6.77
PSS+ *[Cl^-]*//*[NO_2^-]*=1	None	0.1	0.006
PSS+ *[cit]*//*[Cl^-]*=0.5	Pitting	242	13.21
PSS+ *[cit]*//*[Cl^-]*=1	Pitting	412	25.33
PSS + cit	Pitting	319	19.62